ACS APPLIED MATERIALS & INTERFACES

Research Article

www.acsami.org

Electric Field Alignment of Nanofibrillated Cellulose (NFC) in Silicone Oil: Impact on Electrical Properties

Amal Kadimi,[†,‡] Karima Benhamou,[†,§] Zoubeida Ounaies,[‡] Albert Magnin,[∥] Alain Dufresne,*[,§] Hamid Kaddami,*[,†] and Mustapha Raihane[†]

[†]Faculty of Sciences and Technologies, Laboratory of Organometallic and Macromolecular Chemistry-Composite Materials, Cadi Ayyad University, Avenue Abdelkrim Elkhattabi, B.P. 549, Marrakech 40000, Morocco

[‡]Electroactive Materials Characterization Lab, Department of Mechanical & Nuclear Engineering, Pennsylvania State University, 137 Reber Building, University Park, Pennsylvania 16802, United States

[§]The International School of Paper, Print Media and Biomaterials (Pagora), Grenoble Institute of Technology, CS10065, 38402 Saint Martin d'Héres, France

[∥]Laboratoire Rhéologie et Procédés, Grenoble-INP, UJF Grenoble 1, UMR CNRS 5520, BP 53, 38041 Grenoble Cedex 9, France

ABSTRACT: This work aims to study how the magnitude, frequency, and duration of an AC electric field affect the orientation of two kinds of nanofibrillated cellulose (NFC) dispersed in silicone oil that differ by their surface charge density and aspect ratio. In both cases, the electric field alignment occurs in two steps: first, the NFC makes a gyratory motion oriented by the electric field; second, NFC interacts with itself to form chains parallel to the electric field lines. It was also observed that NFC chains become thicker and longer when the duration of application of the electric field is increased. In-situ dielectric properties have shown that the dielectric constant of the medium increases in comparison to the randomly dispersed NFC (when no electric field is applied). The optimal parameters of alignment were found to be 5000 Vpp/mm and 10 kHz for a duration of 20 min for both kinds of NFC. The highest increase in dielectric constant was achieved with NFC oxidized for 5 min (NFC-O-5min) at the optimum conditions mentioned above.

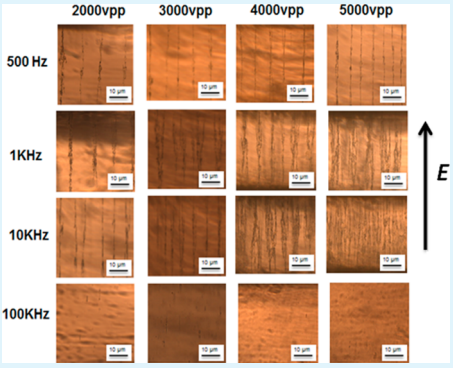

KEYWORDS: *nanofibrillated cellulose (NFC), alignment, electric field, TEMPO-mediated oxidation, extend of oxidation, rachis of palm tree, dielectric permittivity*

INTRODUCTION

Cellulose has the advantage of being both an abundant and a renewable resource. In this β-1,4-linked glucopyranose units based linear polymer, the polymer chains are connected by hydrogen bonds to form microfibrillar aggregates (or bundles of fibrils), along which alternate ordered crystalline and amorphous regions.[1] The extraction of cellulose nanofibers is challenging, but many authors in the literature have succeeded in extracting them from various sources. Cellulose nanocrystals (CNCs) and nanofibrillated cellulose (NFC) are typically the two cellulose nanofibers extracted and characterized. They differ in terms of geometrical characteristics and crystallinity, but in general, NFC has the higher aspect ratio.[2] Recently, many studies dealt with the issue of facilitating NFC extraction. The use of a microfluidizer to apply a mechanical shearing to extract NFC without any prior chemical or enzymatic pretreatment of the pristine cellulose is a high energy demanding process.[3−5] Many studies showed that pretreatment by means of oxidation catalyzed by TEMPO is highly efficient to render the mechanical shearing less energy consuming.[6−8] However, the extent of chemical oxidation has significant effect not only on the surface charge of the produced NFC but also on their geometrical characteristics (such as aspect ratio).[8] The association of NFC and a polymeric matrix enabled production of new nanocomposites with original properties.[3,9−16] The incorporation of NFC brings significant improvement of the mechanical, gas barrier, thermal, and electrical properties. Few papers have been published on the dielectric properties of NFC-based nanocomposites. Recently, the dielectric relaxation of nanocomposites based on NFC-filled rubber has been studied by Ladhar et al.[9] The study showed that the addition of NFC induces new relaxations: one was associated with lignin and hemicelluloses remaining at the surface of NFC, and a second one was due to the interfacial polarization. Also, the dielectric strength increased as a function of the reinforcing phase and then decreased after reaching a threshold value around 7.5 wt % of NFC.

The papers in the literature that dealt with the control and/or characterization of the orientation of cellulose nanofibers in NFC-based materials are numerous. Orientation of cellulose nanofibers is scientifically and technically challenging because it

Received: March 25, 2014
Accepted: May 21, 2014
Published: May 21, 2014

   dx.doi.org/10.1021/am501808h | *ACS Appl. Mater. Interfaces* 2014, 6, 9418−9425

offers valuable opportunities to design new nanocomposites by aligning this nanofiller in polymers to improve dielectric and mechanical properties and can also offer new applications for cellulose valorization. Some studies clearly show that cellulose nanofibers have an orientational self-capacity even if no external solicitation has been applied to improve their orientation.[17−19] Many authors were interested in the control of the orientation of cellulose nanofibers in cellulose nanofiber based materials. The techniques used to orientate NFC were principally mechanical techniques such as cold drawing,[20] shear-convective assembly,[21] electrospinning,[22−25] wet spinning,[26,27] and wet stretching.[28−35]

Some papers dealt with the orientation of cellulose nanofibers usinga magnetic field to process composite materials with controlled structure.[29,36] Although electric field application was widely used to orientate nanoscale inorganic materials,[37−41] only few studies have been dedicated to cellulose nanofibers.[42−44] In order to align cellulose nanocrystals in silicone oil, Kalidindi et al.[42] have used an AC electric field with varying magnitude, frequency, and duration of application. They succeeded in optimizing the chain formation by applying an AC electric field during 20 min at 3000 Vpp mm^{-1} and 500 mHz. They observed that the CNCs rotate before interacting to form chains, and that the chain formation was accompanied by a significant increase of the dielectric constant of the medium (in comparison to the randomly dispersed case). Csoka et al.[30] have succeed in preparing ultrathin films of CNC by applying a low electric field. The setup consisted of a convective assemblage. Their results showed that the orientation of CNC depends on the electric field and frequency. Bordel et al.[43] have succeeded, by mean of AC electric field application, to align native cellulose in organic solvent (chloroform and cyclohexane). They aligned native cellulose at 200 V/mm and 1 kHz alignment frequency and observed rotation of cellulose particles under the electric field. Habibi et al.[44] have tried to align CNCs by means of an AC electric field. They changed the electric field and frequency to investigate the ability to align CNCs in water using a surfactant; they studied the behavior of cellulose for a wide range of voltages (2.5−20 V/mm) in a frequency range from 1 kHz to 2 MHz.

All of the above studies were dedicated to CNC orientation under electric field. We did not find any study in the literature dedicated to the orientation of nanofibrillated cellulose. Except for the work of Sanjay et al., no study reported the effect of the orientation of cellulose nanofibers on the electrical properties of the obtained composites. However, for carbon nanotube based materials many studies have been conducted. A comprehensive study[45] has been conducted to align single-walled carbon nanotubes (SWCNT) by mean of an AC electric field into a polymer matrix obtained by photopolymerization. The authors have shown that it was possible to control the electrical properties of the composite (electrical conductivity and dielectric constant) by varying the AC electric field parameters (magnitude, frequency, and duration of application). Another comprehensive study has been conducted by Sungryul et al.[46] to investigate the alignment of carbon nanotubes in covalently grafted multiwalled carbon nanotubes (MWCNTs) on a cellulose composite. The alignment of MWCNTs contributed to enhance significantly the mechanical and piezoelectric properties. It also improved actuator performance of these composites. Ma et al.[47] have focused on the use of an electric field to study the effect of oxidation on the alignment and dispersion of MWCNTs in in situ polymerized poly(methyl methacrylate) (PMMA) based composites. Their results showed that the dispersion quality as well as the alignment stability was significantly enhanced for oxidized MWCNTs based nanocomposites. Oliva-Avilés et al.,[48] while studying pristine MWCNTs/thermoplastic polymer based nanocomposites, have shown that the alignment of MWCNTs by mean of alternative electric field induced 3−5 orders of magnitude enhancement of the electric conductivity compared to randomly dispersed MWCNTs based nanocomposites.

As mentioned above no study in the literature has been dedicated to the orientation of nanofibrillated cellulose under an electric field and the study of the physical characteristics of NFC on their orientation under the electric field. Therefore, this paper reports a comprehensive study on the relationship between the degree of alignment of NFC in silicone oil and the parameters of the applied electric field (i.e., magnitude, frequency, as well as duration of application). The effect of NFC microstructure, namely, size (length and width), charge, and crystallinity index, on the alignment conditions and dielectric properties was studied.

MATERIALS AND METHODS

Materials. Details about the materials and chemicals used for the TEMPO-catalyzed extraction of NFC can be found in our previously published work.[2] Ethanol, acetone, and *N*,*N*-dimethylformamide (DMF) of analytical grade were purchased from Sigma-Aldrich and used as solvents to disperse the NFC. Silicone oil, used as a dielectric medium, had a cinematic viscosity of 10 mm^2/s and was supplied by Sigma-Aldrich.

Preparation of NFC. The details of the TEMPO-catalyzed oxidation procedure to prepare the oxidized NFC's colloidal suspensions in water are reported in the recently published work of Benhamou et al.[8] Two different oxidation times (5 and 120 min) were chosen to prepare NFC with different physical and geometrical characteristics. Centrifugation at 8500 rpm for 10 min was performed to remove the reagents. The excess liquid was removed from the centrifuge vials with a pipet and replaced with distilled water, and the mixture was homogenized by probe sonication and then centrifuged at 8500 rpm 3 times. After the oxidative pretreatment and reagent removal, a PANDA 2K−GEA-NiroSoaviS laboratory homogenizer was used to perform homogenization. Disintegration by pumping the 2 wt % fiber suspension through the homogenizer was performed up to 15 times at 600 MPa.

The two NFC samples prepared from cellulose oxidized for 5 min and 2 h will be designated in the following as NFC-O-5min and NFC-O-2h, respectively.

Solvent Exchange. To disperse NFC in silicone oil a series of solvent exchanges were performed using successively ethanol, acetone, and DMF (the solvent was removed as a supernatant after the centrifugation step). Finally, the DMF was exchanged with silicone oil. The solvent exchange procedure is described in Figure 1.

Determination of NFC Carboxyl Content by Conductometric Dosage. The carboxyl contents of both studied NFCs were calculated according to the conductometric titration method described by Benhamou et al.[8]

Determination of the Crystallinity Index by X-ray Diffraction Characterization (XRD). The method of preparation of the NFC films for XRD analyses, the characteristics of the X-ray diffractometer, and the parameter of XRD experiments are similar to those described in our previous work.[8] The Segal method[49] was used to estimate the crystallinity index (CI):

$$\mathrm{CI} = I_{002} - I_{\mathrm{am}}/I_{002} \times 100 \quad (1)$$

where I_{002} is the height of the 002 pic (2θ in the range 22−23°) and I_{am} is the lower value at 2θ in the range 18−19°, corresponding to the X-ray intensity reflected by the amorphous domains.

Estimation of the Degree of Polymerization of Cellulose. The average intrinsic viscosity value was used to estimate the degree of polymerization (DP) of cellulose chains forming NFC. The relationship

dx.doi.org/10.1021/am501808h | ACS Appl. Mater. Interfaces 2014, 6, 9418−9425

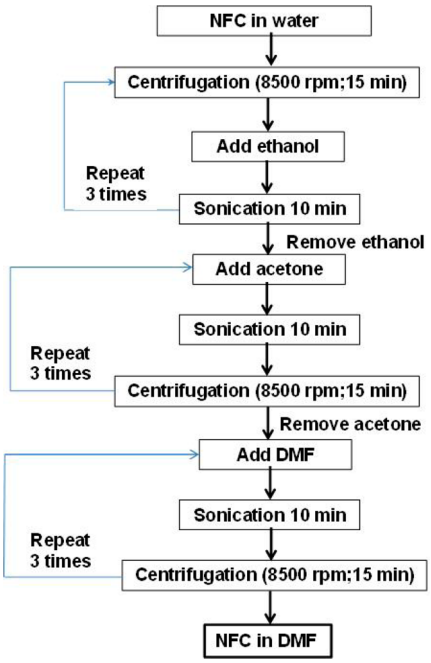

Figure 1. Flowchart showing the steps of solvent exchange.

between the intrinsic viscosity, $[\eta]$ (dL/g), and DP proposed for cellulose by Rinaudo[50] was used to calculate DP from measurements of $[\eta]$:

$$[\eta] = 0.891\mathrm{DP}^{0.936} \quad (2)$$

Cupri-ethylendiamine (1 N) was used as the solvent for NFC. At least three solutions of different concentrations were prepared to determine $[\eta]$ (dL/g). The measurements were performed at 25 ± 0.1 °C, and an average of three measurements of the flow time was used to calculate the intrinsic viscosity. The intrinsic viscosity of bleached cellulose was calculated and served as reference.

Atomic Force Microscopy (AFM). A Nanoscope III (Veeco Co. Ltd., USA) was used to perform AFM observations. An aqueous suspension (0.01 wt %) was sonicated for 30 min to allow better dispersion of NFC. The samples for AFM characterization were prepared by depositing drops of the sonicated NFC dispersion onto the mica substrates and thereafter air drying the sample at ambient conditions. Silicon cantilevers were used for the in air tapping mode to record all AFM micrographs. The tapping was performed at the frequency range of 264−339 kHz and with radius of curvature between 10 and 15 nm. The NFC dimensions, including length (L) and width (W), were measured by using Nanoscope software. An average of more than 100 measurements performed on individual nanofibrils statistically chosen and analyzed was calculated and used to determine length and width distribution (mainly focusing on the images with the scale of 3.3 μm × 3.3 μm).

Electric Field Processing. A 0.1 wt % solution of NFC was dispersed in silicone oil (as mentioned above). The dispersion (NFC-silicone oil) was then poured into the gap between the parallel electrodes glued on a glass microscope slide (shown in Figure 2).

The gap size between the electrodes was set to 1 mm. Frequencies ranging from 500 Hz to 100 kHz were used to apply the AC electric field. The AC signal was generated using a HP 33120A. This later was connected with a TREK 609D-6 high voltage amplifier to adjust the voltage. The electric field magnitudes applied for the alignment experiments were 2000, 3000, 4000, and 5000 Vpp/mm.

Optical Microcopy. The optical microscopy procedure is described in our earlier published work.[42]

Dielectric Spectroscopy. The measurement of the in situ dielectric constant was performed at ambient conditions using a Quadtech LCR meter. A wide range of frequencies from 500 Hz to 1 MHz were explored. This technique yields capacitance, which was then converted

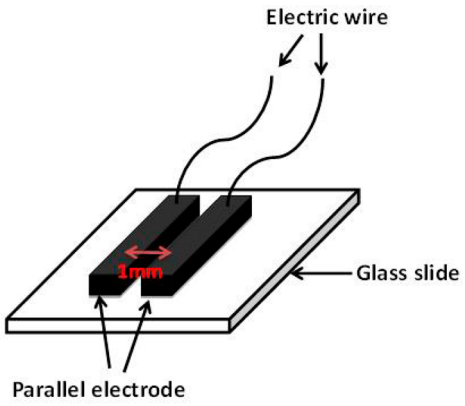

Figure 2. Schematic of parallel electrodes configuration setup. The distance between the electrodes is 1 mm.

to dielectric permittivity using eq 3, assuming a parallel plate configuration:

$$\varepsilon = \frac{Cd}{\varepsilon_0 A} \quad (3)$$

where C = capacitance (in F), ε = dielectric constant, ε_0 = permittivity of free space (in F m^{-1}), d = distance between electrodes (in m), and A = surface of the electrodes (in m^2).

RESULTS AND DISCUSION

NFC Characterization. AFM images of the oxidized NFC showed that the nanofibrils clearly differed in width and length, depending on the extent of the oxidative treatment (Figure 3A and B). More than 100 nanofibrils on AFM images for each oxidized NFC sample were used to measure width and length distribution using Nanoscope Analysis-III software. The width of NFC-O-5min ranged from 20 to 40 nm, while NFC-O-2h displayed a narrow width distribution from 10 to 18 nm. The lower width of the NFC-O-2h is the result of pronounced defibrillation resulting from the repulsive forces between the adjacent sodium carboxylate groups existing at their surface. Increasing the density of these charged groups results in stronger repulsive force intensity, and the NFC aggregation is reduced.[7]

The reduction of the fiber length is the result of cellulose molecule chain depolymerization through β-elimination. This reduction was confirmed by molecular degree of polymerization measurements (see Table 1). The reactive species such as hydroxide anion and/or radical species created in situ are expected to be responsible for the side reactions leading to the cleaving of (1−4)-β-glycoside links during the TEMPO-catalyzed oxidation.[8]

Electric Field Manipulation of NFCs. Optical microscopy (OM) images showed the predispersion of NFC in silicone oil (Figure 4). No nanofiber could be observed, which means that NFC was dispersed at the nanoscale.

Figures 5 and 6 show how the frequency and the electric field magnitude affect the alignment and chain formation for both kinds of NFC. The OM images show the dispersion status of NFC after application of the AC electric field and testify that alignment of NFCs was obtained. AC electric fields of 2000, 3000, 4000, and 5000 Vpp/mm were applied at varying frequencies (500 Hz to 100 kHz). For all frequencies we observed that NFC rotated and aligned in the direction of the electric field.

The action of the electric field can be considered to act in two steps: first, the nanofibers make a gyratory motion oriented by

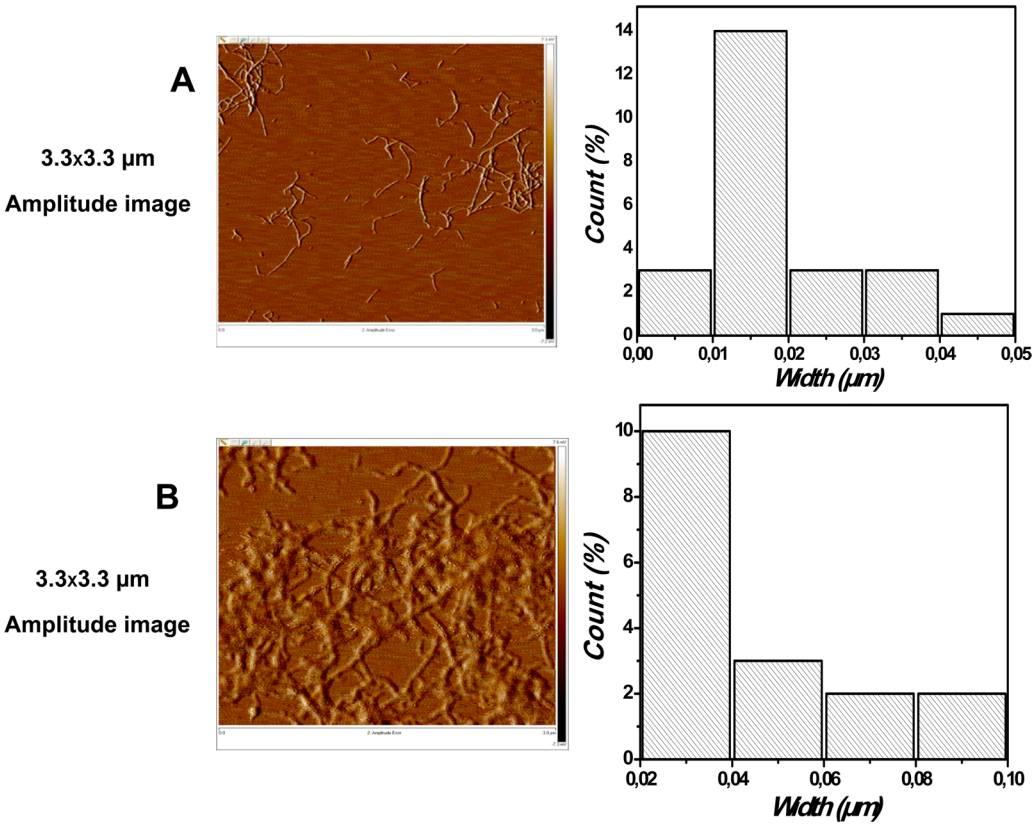

Figure 3. AFM images and their corresponding measured width distributions (histograms at the right of the AFM images) for (A) NFC-O-2h and (B) NFC-O-5min.

Table 1. Characteristics of NFC

sample	size[a]	dp[b]	COO^-Na^+ content (μmol/g)
NFC-O-5min	L = 0.55 μm; W = 20−40 nm	500	221
NFC-O-2h	L = 0.11 μm; W = 10−18 nm	100	774

[a]L = length, W = width. [b]Degree of polymerization.

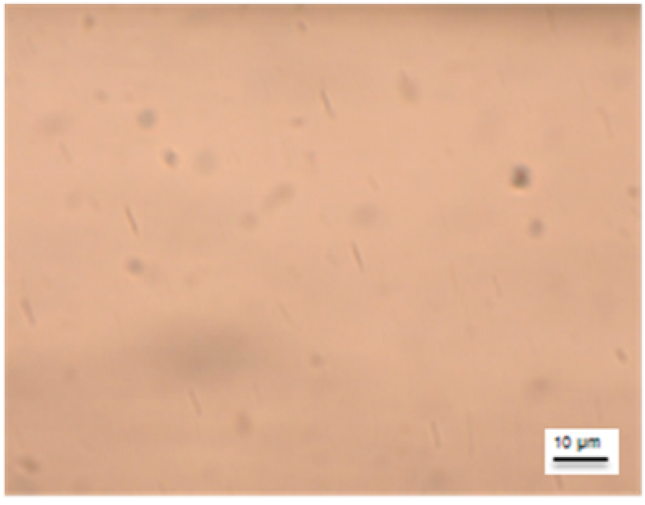

Figure 4. Image of the initial dispersion of NFC in silicone oil obtained from OM observations (before application of electric field).

the electric field for 10 Hz to 100 kHz applied frequencies (see Figures 5 and 6). When an alternating electric field was applied to

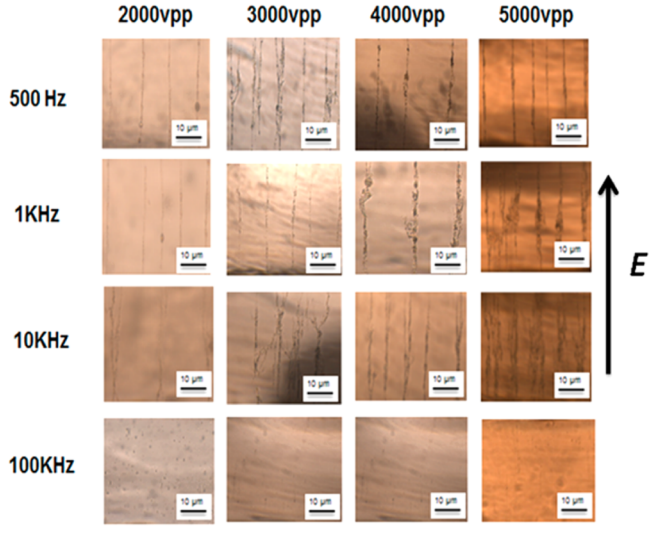

Figure 5. Alignment and chain formation of NFC-O-2h in silicone oil as a function of frequency and magnitude of the electric field. The scale bar in all images is 10 μm, and the electric field direction is indicated by the vertical arrow.

the particle, the NFC was polarized. Due to the anisotropic polarizability of NFC, the interaction between the dipoles of the polarized particles and the imposed electric field is governed by a rotation mechanism. The corresponding effect is called dielectrophoretic (DEP) force. The dielectrophoretic effect also leads to patterning when the particle concentration between the electrodes is high. The AC field induces dipoles within the particles that interact with each other, resulting in a "chaining"

dx.doi.org/10.1021/am501808h | ACS Appl. Mater. Interfaces 2014, 6, 9418−9425

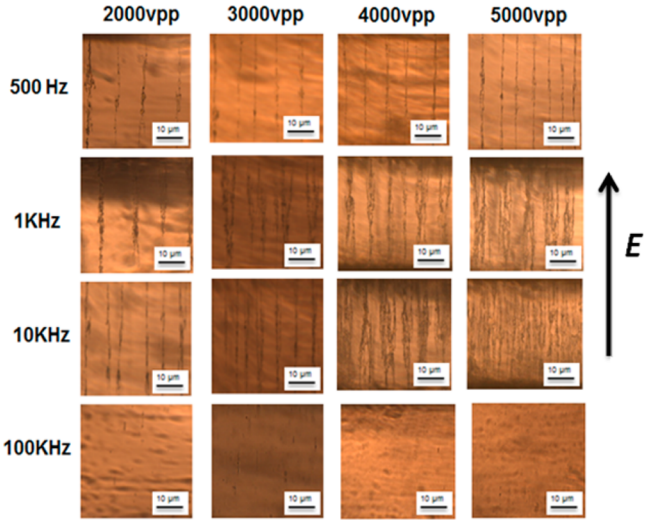

Figure 6. Alignment and chain formation of NFC-O-5min in silicone oil as a function of frequency and magnitude of the electric field. The scale bar in all images is 10 μm, and the electric field direction is indicated by the vertical arrow.

force.[51] This latter forces the particles to align in chains along the field lines; therefore, the second step involves the formation of chains. The phenomenon of dieletrophoresis is the motion induced on a dielectric particle by mean of a nonuniform electric field.[52] The combination of NFC gyration and chaining in the field direction resulted in the manifested effects. In our approach, the suspension of NFC in silicone oil was subjected to the effect of a uniform AC electric field. This latter induces the polarization of the NFC and, under the effect of the dielectrophoretic force (DEP), causes their attraction toward high field intensity regions. Chaining occurrence and intensity were dependent on the frequency, which indicates that the driving force is dielectrophoresis.[41,53,54] The Clausius−Mossoti factor, which governs the dielectrophoretic force, is dependent on the dielectric permittivity of NFC and the dispersion medium (silicone oil). This factor is therefore dependent on the frequency, and accordingly, the dielectrophoretic force varies as the alignment frequency is changed.

For all frequencies except 100 kHz we observe that after just 5 min of electric field application the particles start forming very thin chains. For 10 min the particles form thin chains that are denser than the chains formed after 5 min. The thin chains congregate to form denser and highly thicker ones. Beyond 20 min, no improvement in chain size or in alignment was observed. Monitoring the formation of chains was also conducted by measuring the change of the permittivity of the medium vs time. No improvement of the dielectric constant of the medium was observed after that time. Thus, 20 min corresponds to the optimal time for alignment. We could then conclude that in addition to the electric field magnitude and the frequency, time is the third parameter that affects the NFC alignment. At 100 kHz, NFC aligned but no chain formation could be observed.

This result is consistent with the reported observations.[41,54] Some studies have shown that under an AC field of high frequency, the mobile charges could not respond to applied electric field because they have insufficient time to achieve that. On the other hand, the magnitude of the field gradient is too small to extend so far from the edge of the electrode.[30,55] However, Moscatello et al.[54] reported that it is very hard to determine the role of frequency, and it is not clear why the chain formation and their density decrease at higher frequencies.

In fact, the chain formation leads to an increase of the medium permittivity. The bigger and denser the chains are, the higher the dielectric constant becomes. After 20 min the chains reach the highest possible size, and the medium permittivity reaches a constant value (see examples in Figure 7). The influence of chain

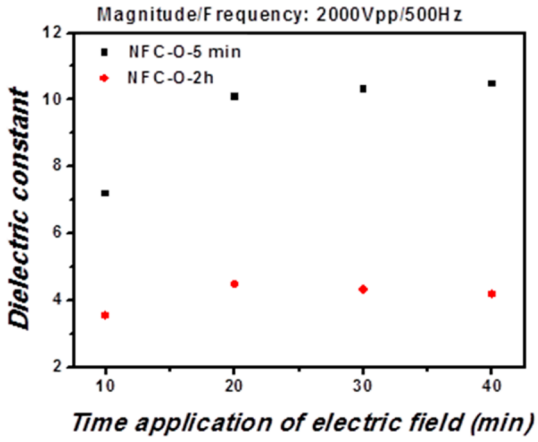

Figure 7. In situ dielectric constant at 1 kHz vs time (magnitude of the applied field, 2000 Vpp/mm; frequency, 500 Hz).

formation on dielectric constant have been investigated by Kalidindi et al.[42] and Li,[53] when studying the alignment under electric field of CNC and barium titanate nanoparticles, respectively. Both reported that the thick chains contribute to the largest increase in dielectric constant, which is consistent with our results.

To investigate the effect of NFC characteristics on the alignment and chaining, in situ permittivity of the NFC dispersions in silicone oil was characterized. The permittivity was measured in the alignment direction. These measurements were performed after 20 min of electric field application. Four different electric field magnitudes have been used for a large frequency range from 500 Hz to 100 kHz. The results obtained for the dielectric constant for both types of NFC are showed in Figure 8A and B. The dielectric constant of the suspension without applying the AC electric field (random case) at 1 kHz was found to be 2.8 for NFC-O-2h and 4.5 for NFC-O-5min.

For NFC-O-2h (Figure 8B), at 2000 Vpp/mm no significant improvement in dielectric constant in comparison to the "randomly dispersed" case was observed. At 3000, 4000, and 5000 Vpp/mm we observed a significant improvement in the medium permittivity as a function of voltage applied, especially for 5000 Vpp/mm at 10 kHz giving a value of 8.3, mirroring the alignment behavior shown in Figure 5 (at 10 kHz 5000 Vpp exhibiting the thicker and highly dense chain), further confirming that the dimensions of the formed chains have significant impact on these properties. In the case of NFC-O-5min, Figure 8A shows a significant improvement in the dielectric constant for all voltages in comparison to the "randomly dispersed" case; the optimal parameters were found to be 5000 Vpp/mm and 10 kHz. It is found that the dielectric constant increases in these conditions from 4.5 to 14.8.

Significant difference in dielectric constant was observed between NFC-O-5min and NFC-O-2h, either in random or aligned case (Figures 9A and B). This difference could be linked to the quantity and density of chains formed for each type of

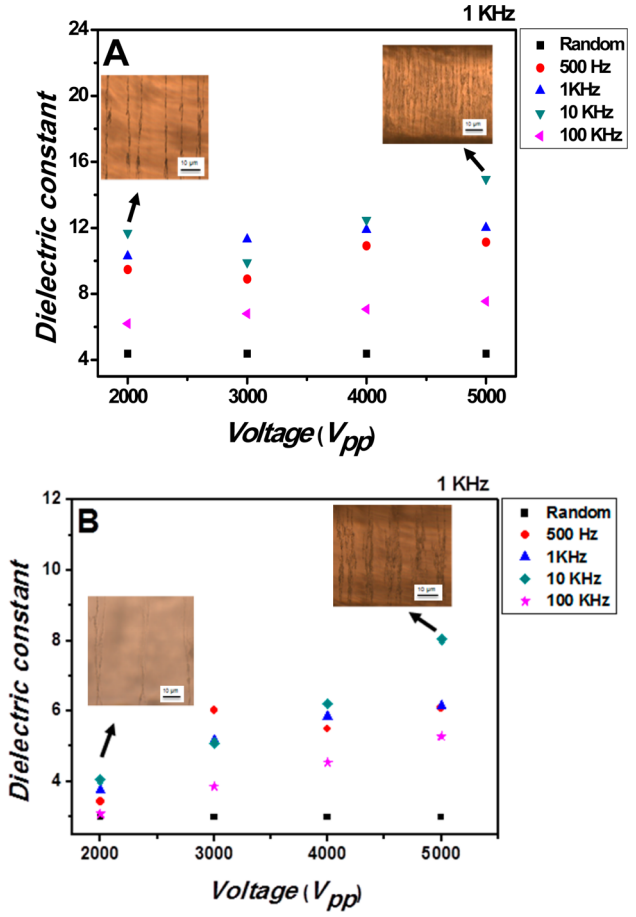

Figure 8. In situ dielectric constant vs applied voltage at the frequency of measurement of 1 kHz for different frequencies of external applied electric field: (A) NFC-O-5min and (B) NFC-O-2h. OM images showed the density of chains formed after 20 min of application of electric field (magnitude, 2000 and 5000 Vpp/mm; frequency of applied field, 10 kHz) for both types of NFC.

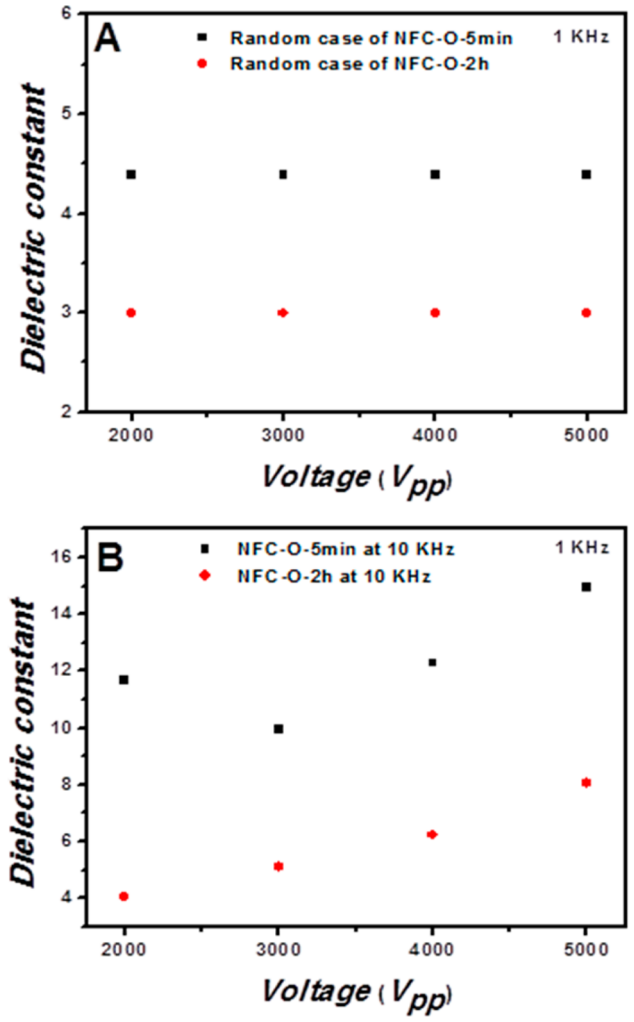

Figure 9. In situ dielectric constant at 1 kHz (frequency of measurement) as a function of magnitude (from 2000 to 5000 Vpp/mm) and frequency of applied electric field 10 kHz: (A) randomly dispersed NFC in silicone oil and (B) aligned NFC.

NFC in similar alignment conditions. In fact, it was found that the application of an AC electric field can enhance the dielectric constant and density of chain formation for both NFC, but NFC-O-5min exhibits the thicker and more highly dense chain and also higher dielectric constant of ~14.8 (compared to the higher dielectric constant obtained for NFC-O-2h, which is about 8). These variations of dielectric constant and chain density formation can be understood by the higher surface charge of the NFC-O-2h (carboxylic content (774 μmol/g) compared to NFC-O-5min (221 μmol/g)). The existence of considerable amounts of negative surface charges on the NFC-O-2h surface may cause the formation of thin chains resulting from repulsive interactions between these negative charges and enable them to repel each other and prevent the formation of numerous and dense chains.

In addition to the surface charges of NFC, the size seems to be an important parameter that could influence its alignment. In fact, some studies on the alignment under an electric field have shown that the size of CNT influences their alignment under an electric field. Jang and Sakka[56] observed that small width CNT below 20 nm were not well aligned compared to CNT with a width of about 40 nm. On the other hand, Abhishek et al.,[57] while comparing the alignment under AC electric field of thick and thin GaN nanowires, found that the thicker ones undergo larger DEP force and consequently show higher probability of alignment.

CONCLUSION

Aiming to investigate the orientation of nanofibrillated cellulose (NFC) in silicone oil, NFC was extracted from date palm tree rachis, which was oxidized by TEMPO (2,2,6,6-tetramethylpiperidine-1-oxyl) for 5 min or 2 h. First, we focused on the characterization of both kinds of NFC by AFM and determined the carboxyl content of oxidized cellulose and the degree of polymerization of cellulose chains forming NFC. Second, we focused on the examination of the behavior of NFC in silicone oil under the effect of an AC electric field. Three parameters were changed: the AC electric field magnitude, its frequency, and the duration of application. The presented results showed that the orientation of both types of NFC was successfully attained. The optimal parameters of alignment for both NFC samples (NFC-O-5min and NFC-O-2h) were found to be 5000 Vpp/mm and 10 kHz for duration of 20 min.

Under the applied electric field NFC responds in a two-step process: in the first step, the dipoles of the polarized particles interact with the imposed electric field governing a gyration mechanism caused by the anisotropic of NFC. The corresponding effect is called dielectrophoretic (DEP) force, which also leads to the structuring at higher particle concentrations between

dx.doi.org/10.1021/am501808h | ACS Appl. Mater. Interfaces 2014, 6, 9418−9425

the electrodes reacting as dipoles by AC fields interact with each other, resulting in a "chaining" force. The particles align in chains along the electric field lines; therefore, chains of particles are formed in the direction of the electric field, in the second step. In situ dielectric properties were used to study the influence of the alignment of NFC in silicone oil on the dielectric constant. The dielectric constant was measured to qualify and characterize the alignment of NFC. Our dielectric results for both types of NFC indicated that the alignment conditions, such as frequency, magnitude, and application duration of the applied electric field, have substantial impact on the dielectric properties.

AUTHOR INFORMATION

Corresponding Authors

*E-mail: alain.dufresne@pagora.grenoble-inp.fr.
*E-mail: h.kaddami@uca.ma.

Notes

The authors declare no competing financial interest.

ACKNOWLEDGMENTS

The authors thank for their financial supports the Hassan II Academy of Science and Technology, the International Institute for Multifunctional Materials for Energy Conversion-IIMEC (Texas, USA), and The CNRST-Morocco/CNRS-France (Volubilis Project).

REFERENCES

(1) Azizi Samir, M. A. S.; Alloin, F.; Dufresne, A. Review of Recent Research into Cellulosic Whiskers, their Properties and their Application in Nanocomposite Field. *Biomacromolecules* **2005**, *6*, 612−626.

(2) Dufresne, A. *Nanocellulose: From nature to high performance tailored materials*; Walter de Gruyter GmbH: Berlin/Boston, 2012.

(3) Bendahou, A.; Kaddami, H.; Dufresne, A. Investigation on the Effect of Cellulosic Nanoparticles Morphology on the Properties of Natural Rubber Based Nanocomposites. *Eur. Polym. J.* **2010**, *46*, 609−620.

(4) Turbak, A. F.; Snyder, F. W.; Sandberg, K. R. Microfibrillated Cellulose, a New Cellulose Product: Properties, Uses and Commercial Potential. *J. Appl. Polym. Sci.: Appl. Polym. Symp.* **1983**, *37*, 815−827.

(5) Herrick, F. W.; Casebier, R. L.; Hamilton, J. K.; Sandberg, K. R. Microfibrillated Cellulose: Morphology and Accessibility. *J. Appl. Polym. Sci.: Appl. Polym. Symp.* **1983**, *37*, 797−813.

(6) Besbes, I.; Alila, S.; Boufi, S. Nanofibrillated Cellulose from TEMPO-Oxidized Eucalyptus Fbres: Effect of the Carboxyl Content. *Carbohydr. Polym.* **2011**, *84*, 975−983.

(7) Isogai, A.; Saito, T.; Fukuzumi, H. TEMPO-Oxidized Cellulose Nanofibers. *Nanoscale* **2011**, *3*, 71−85.

(8) Benhamou, K.; Dufresne, A.; Magnin, A.; Mortha, G.; Kaddami, H. Control of Size and Viscoelastic Properties of Nanofibrillated Cellulose from Palm Tree by Varying the TEMPO-Mediated Oxidation Time. *Carbohydr. Polym.* **2014**, *99*, 74−83.

(9) Ladhar, A.; Arous, M.; Kaddami, H.; Raihane, M.; Lahcini, M.; Kallel, A.; Graca, M. P. F.; Costa, L. C. Dielectric Relaxation Studies on Nanocomposite of Rubber with Nanofibrillated Cellulose. *J. Non-Cryst. Solids* **2013**, *378*, 39−44.

(10) Trovatti, E.; Fernandes, S. C. M.; Rubatat, L.; da Silva Perez, D.; Freire, C. S. R.; Silvestre, A. J. D.; Neto, C. P. Pullulan-Nanofibrillated Cellulose Composite Films with Improved Thermal and Mechanical Properties. *Compos. Sci. Technol.* **2012**, *72*, 1556−1561.

(11) Endo, R.; Saito, T.; Isogai, A. TEMPO-Oxidized Cellulose Nanofibril/Poly(Vinyl Alcohol) Composite Drawn Fibers. *Polymer* **2012**, *54*, 935−941.

(12) Larsson, K.; Berglund, L. A.; Ankerfors, M.; Lindström, T. Polylactide Latex/ Nanofibrillated Cellulose Bionanocomposites of High Nanofibrillated Cellulose Content and Nanopaper Network Structure Prepared by a Papermaking Route. *J. Appl. Polym. Sci.* **2012**, *125*, 2460−2466.

(13) Seydibeyoğlu, M. O.; Oksman, K. Novel Nanocomposites Based on Polyurethane and Micro Fibrillated Cellulose. *Compos. Sci. Technol.* **2007**, *68*, 908−914.

(14) Jonoobi, M.; Harun, J.; Mathew, A. P.; Oksman, K. Mechanical Properties of Cellulose Nanofiber (CNF) Reinforced Polylactic Acid (PLA) Prepared by Twin Screw Extrusion. *Compos. Sci. Technol.* **2010**, *70*, 1742−1747.

(15) Fernandes, S. C. M.; Freire, C. S. R.; Silvestre, A. J. D.; Neto, C. P.; Gandini, A.; Berglund, L. A.; Salmén, L. Transparent Chitosan Films Reinforced with a High Content of Nanofibrillated Cellulose. *Carbohydr. Polym.* **2010**, *81*, 394−401.

(16) Suryanegara, L.; Nakagaito, A. N.; Yano, H. The Effect of Crystallization of PLA on the Thermal and Mechanical Properties of Microfibrillated Cellulose-Reinforced PLA Composites. *Compos. Sci. Technol.* **2009**, *69*, 1187−1192.

(17) Uetani, K.; Yano, H. Self-Organizing Capacity of Nanocelluloses via Droplet Evaporation. *Soft Matter* **2013**, *9*, 3396−3401.

(18) Habibi, Y.; Foulon, L.; Aguié-Béghin, V.; Molinari, M.; Douillard, R. Langmuir−Blodgett Flms of Cellulose Nanocrystals: Preparation and Characterization. *J. Colloid Interface Sci.* **2007**, *316*, 388−397.

(19) Pullawan, T.; Wilkinson, A. N.; Zhang, L.; Eichhorn, S. J. Deformation Micromechanics of All-Cellulose Nanocomposites: Comparing Matrix and Reinforcing Components. *Carbohydr. Polym.* **2013**, *100*, 31−39.

(20) Sehaqui, H.; Mushi, N. E.; Morimune, S.; Salajkova, M.; Nishino, T.; Berglund, L. A. Cellulose Nanofiber Orientation in Nanopaper and Nanocomposites by Cold Drawing. *ACS Appl. Mater. Interfaces* **2012**, *4*, 1043−1049.

(21) Khelifa, F.; Habibi, Y.; Leclère, P.; Dubois, P. Convection-Assisted Assembly of Cellulose Nanowhiskers Embedded in an Acrylic Copolymer. *Nanoscale* **2013**, *5*, 1082−1090.

(22) Peresin, M. S.; Habibi, Y.; Zoppe, J. O.; Pawlak, J. J.; Rojas, O. J. Nanofiber Composites of Polyvinyl Alcohol and Cellulose Nanocrystals: Manufacture and Characterization. *Biomacromolecules* **2010**, *11*, 674−681.

(23) Andersson, R. L.; Salajkova, M.; Mallon, P. E.; Berglund, L. A.; Hedenqvist, M. S.; Olsson, R. T. Micromechanical Tensile Testing of Cellulose-Reinforced Electrospun Fibers Using a Template Transfer Method (TTM). *J. Polym. Environ.* **2012**, *20*, 967−975.

(24) Sehaqui, H.; Morimune, S.; Nishino, T.; Berglund, L. A. Stretchable and Strong Cellulose Nanopaper Structures Based on Polymer-Coated Nanofiber Networks: an Alternative to Nonwoven Porous Membranes from Electrospinning. *Biomacromolecules* **2012**, *13*, 3661−3667 (2012).

(25) Dong, H.; Strawhecker, K. E.; Snyder, J. F.; Orlicki, J. A.; Reiner, R. S.; Rudie, A. W. Cellulose Nanocrystals as a Reinforcing Material for Electrospun Poly(Methyl Methacrylate) Fbers: Formation, Properties and Nanomechanical Characterization. *Carbohydr. Polym.* **2012**, *87*, 2488−2495.

(26) Endo, R.; Saito, T.; Isogai, A. TEMPO-Oxidized Cellulose Nanofibril/Poly(Vinyl Alcohol) Composite Drawn Fbers. *Polymer* **2012**, *54*, 935−941.

(27) Iwamoto, S.; Isogai, A.; Iwata, T. Structure and Mechanical Properties of Wet-Spun Fibers Made from Natural Cellulose Nanofibers. *Biomacromolecules* **2011**, *12*, 831−836.

(28) Pullawan, T.; Wilkinson, A. N.; Eichhorn, S. J. Orientation and Deformation of Wet-Stretched All-Cellulose Nanocomposites. *J. Mater. Sci.* **2013**, *48*, 7847−7855.

(29) Pullawan, T.; Wilkinson, A. N.; Eichhorn, S. J. Influence of Magnetic Field Alignment of Cellulose Whiskers on the Mechanics of All-Cellulose Nanocomposites. *Biomacromolecules* **2012**, *13*, 2528−2536.

(30) Csoka, L.; Hoeger, I. C.; Peralta, P.; Peszlen, I.; Rojas, O. J. Dielectrophoresis of Cellulose Nanocrystals and Alignment in Ultrathin Films by Electric Field-Assisted Shear Assembly. *J. Colloid Interface Sci.* **2011**, *363*, 206−212.

(31) Pahimanolis, N.; Salminen, A.; Penttilä, P. A.; Korhonen, J. T.; Johansson, L. S.; Ruokolainen, J.; Serimaa, R.; Seppälä, J. Nanofibrillated Cellulose/Carboxymethyl Cellulose Composite with Improved Wet Strength. *Cellulose* **2013**, *20*, 1459−1468.
(32) Rosilo, H.; Kontturi, E.; Seitsonen, J.; Kolehmainen, E.; Ikkala, O. Transition to Reinforced State by Percolating Domains of Intercalated Brush-Modified Cellulose Nanocrystals and Poly(Butadiene) in Cross-Linked Composites Based on Thiol-Ene Click Chemistry. *Biomacromolecules* **2013**, *14*, 1547−1554.
(33) Sano, M. B.; Rojas, A. D.; Gatenholm, P.; Davalos, R. V. Electromagnetically Controlled Biological Assembly of Aligned Bacterial Cellulose Nanofibers. *Ann. Biomed. Eng.* **2010**, *38*, 2475−2484.
(34) Chulho, Y.; Jung-Hwan, K.; Joo-Hyung, K.; Jaehwan, K.; Heung, S. K. Piezoelectricity of Wet Drawn Cellulose Electro-Active Paper. *Sens. Actuators A* **2009**, *154*, 117−122.
(35) Nishiyama, Y.; Kuga, S.; Wada, M.; Okano, T. Cellulose Microcrystal Film of High Uniaxial Orientation. *Macromolecules* **1997**, *30*, 6395−6397.
(36) Kim, J.; Chen, Y.; Kang, K. S.; Park, Y. B.; Schwartz, M. Magnetic Field Effect for Cellulose Nanofiber Alignment. *J. Appl. Phys.* **2008**, *104*, 096104.
(37) Liu, S.; Li, R.; Zhou, J.; Zhang, L. Effects of External Factors on the Arrangement of Plate-Liked Fe2O3 Nanoparticles in Cellulose Scaffolds. *Carbohydr. Polym.* **2012**, *87*, 830−838.
(38) Lisjak, D.; Ovtar, S. The Alignment of Barium Ferrite Nanoparticles from Their Suspensions in Electric and Magnetic Fields. *J. Phys. Chem. B* **2013**, *117*, 1644−1650.
(39) Chen, Z.; Yang, Y.; Chen, F.; Qing, Q.; Wu, Z.; Liu, Z. Controllable Interconnection of Single-Walled Carbon Nanotubes under AC Electric Field. *J. Phys. Chem. B* **2005**, *109*, 11420−11423.
(40) Shi, D.; He, P.; Zhao, P.; Guo, F.; Wang, F.; Huth, C.; Chaud, X.; Bud'ko, S. L.; Lian, J. Magnetic Alignment of Ni/Co-Coated Carbon Nanotubes in Polystyrene Composites. *Composites, Part B* **2011**, *42*, 1532−1538.
(41) Dan, B.; Wingfield, T. B.; Evans, J. S.; Mirri, F.; Pint, C. L.; Pasquali, M.; Smalyukh, I. I. Templating of Self-Alignment Patterns of Anisotropic Gold Nanoparticles on Ordered SWNT Macrostructures. *ACS Appl. Mater. Interfaces* **2011**, *3*, 3718−3724.
(42) Kalidindi, S.; Ounaies, Z.; Kaddami, H. Toward the Preparation of Nanocomposites with Oriented Fillers: Electric Field-Manipulation of Cellulose Whiskers in Silicone Oil. *Smart Mater. Struct.* **2010**, *19*, 094002.
(43) Bordel, D.; Putaux, J. L.; Heux, L. Orientation of Native Cellulose in an Electric Field. *Langmuir* **2012**, *22*, 4899−4901.
(44) Habibi, Y.; Heim, T.; Douillard, R. AC Electric Field-Assisted Assembly and Alignment of Cellulose Nanocrystals. *J. Polym. Sci., Part B: Polym.,Phys.* **2008**, *46*, 1430−1436.
(45) Park, C.; Wilkinson, J.; Banda, S.; Ounaies, Z.; Wise, K. E.; Sauti, G.; Lillehei, P. T.; Harrison, J. S. Aligned Single-Wall Carbon Nanotube Polymer Composites Using an Electric Field. *J. Polym. Sci., Part B: Polym. Phys.* **2006**, *44*, 1751−1762.
(46) Yun, S.; Kim, J. Mechanical, Electrical, Piezoelectric and Electro-Active Behavior of Aligned Multi-Walled Carbon Nanotube/Cellulose Composites. *Carbon* **2010**, *49*, 518−527.
(47) Ma, C.; Zhang, W.; Zhu, Y.; Ji, L.; Zhang, R.; Koratkar, N.; Liang, J. Alignment and Dispersion of Functionalized Carbon Nanotubes in Polymer Composites Induced by an Electric Field. *Carbon* **2008**, *46*, 706−720.
(48) Oliva-Avilés, A. I.; Avilés, F.; Sosa, V. Electrical and Piezoresistive Properties of Multi-Walled Carbon Nanotube/Polymer Composite Films Aligned by an Electric Field. *Carbon* **2011**, *49*, 2989−2997.
(49) Segal, L.; Creely, J. J.; Martin, A. E.; Conrad, C. M. An Empirical Method for Estimating the Degree of Crystallinity of Native Cellulose Using the X-Ray diffractometer. *Text. Res. J.* **1959**, *29*, 786−794.
(50) Rinaudo, M. Etude Physico-Chimique des Solutions de Cellulose dans le FeTNa. *Papeterie* **1968**, *90*, 479−487.
(51) Velev, O. D.; Gangwal, S.; Petsev, D. N. Particle-Localized AC and DC Manipulation and Electrokinetics. *Ann. Rep. Prog. Chem. Sect. C* **2009**, *105*, 213−246.
(52) Pohl, H. A.; Crane, J. S. Dielectrophoresis of Cells. *Biophys. J.* **1971**, *11*, 711−727.
(53) Li, J. Synthesis and Electric Field-Manipulation of High Aspect Ratio Barium Titanate. Ph.D. Thesis, Texas A&M University, USA, 2011.
(54) Moscatello, J.; Kayastha, V.; Pandey, A.; Ulmen, B.; Yap, Y. K. Dielectrophoretic Deposition of Carbon Nanotubes with Controllable Density and Alignment. *Mater. Res. Soc. Symp. Proc.* **2008**, *1057*, 1−6.
(55) Shaofan, L.; Dong, Q. *Multiscale Simulations and Mechanics of Biological Materials*; John Wiley & Sons: Chichester, U.K., 2013.
(56) Jang, B. K.; Sakka, Y. Influence of Shape and Size on the Alignment of Multi-Wall Carbon Nanotubes Under Magnetic Fields. *Mater. Lett.* **2009**, *63*, 2545−2547.
(57) Motayed, A.; He, M.; Davydov, A. V.; Melngailis, J.; Mohammad, S. N. Realization of Reliable GaN Nanowire Transistors Utilizing Dielectrophoretic Alignment Technique. *J. Appl. Phys.* **2006**, *100*, 114310−114319.